Stability of the shape of a surfactant-laden drop translating at low Reynolds number

Robert A. Johnson and Ali Borhan[a)]
Department of Chemical Engineering, The Pennsylvania State University, University Park, Pennsylvania 16802-4400

(Received 15 July 1999; accepted 30 November 1999)

We examine the effect of surfactants on the evolution of the shape of an initially nonspherical drop translating in an otherwise quiescent fluid at low Reynolds number. A combination of the boundary-integral method and a finite-difference scheme is used to solve the coupled fluid dynamics and surfactant transport problems, in conjunction with the Frumkin adsorption framework to account for the effects of monolayer saturation and nonideal surfactant interactions. For sufficiently small Bond numbers, the drop achieves a nonspherical steady shape. For large initial deformations or Bond numbers, however, the drop deforms continuously, and eventually breaks up through either the formation of an elongated tail or the development of a re-entrant cavity at the trailing end, similar to the mechanisms of drop breakup reported by Koh and Leal [Phys. Fluids A **1**, 8 (1989)], and Pozrikidis [J. Fluid Mech. **210**, 1 (1990)], for surfactant-free drops. Surfactants are found to have a destabilizing effect on the shape of translating drops. The destabilizing effect is mitigated by the presence of strongly-cohesive surfactant interactions, and by surfactant transport between the bulk and the interface. © *2000 American Institute of Physics.* [S1070-6631(00)02503-4]

I. INTRODUCTION

The motion of a droplet translating through an unbounded Newtonian fluid domain has been extensively studied in the past (cf. Clift *et al.*[1]). Hadamard and Rybzynski independently analyzed the free rise/fall of a spherical droplet in the creeping flow limit, and found the following expression for the terminal velocity, U_{HR}, of the droplet:

$$U_{\mathrm{HR}}=\frac{2(\lambda+1)}{3(3\lambda+2)}, \tag{1}$$

where λ is the ratio of the drop phase viscosity to the suspending fluid viscosity. Taylor and Acrivos[2] later showed that a sphere is an exact solution for the steady drop shape in the zero Reynolds number limit, and that the introduction of small inertial effects causes the drop to deform into an oblate ellipsoid. The *stability* of the shape of a spherical drop falling freely in an unbounded domain was first examined by Kojima *et al.*[3] who showed that, in the zero interfacial tension limit, the spherical shape is unstable to infinitesimal perturbations, with a growth rate for the instability which scales as $(1+\lambda)^{-1}$. The nonlinear stability of a translating drop to finite shape perturbations was subsequently studied by Koh and Leal,[4,5] and Pozrikidis.[6] These authors found two modes of instability for the buoyancy-driven translation of drops: the formation of a continuously elongating tail at the rear stagnation point of drops that are initially perturbed into a prolate ellipsoid, and the development of a growing re-entrant cavity at the trailing end of initially-oblate drops. A summary of these stability results is provided in the review article by Stone.[7]

The results of the aforementioned studies are applicable only to 'clean' two-phase systems (i.e., in the absence of surface-active species). Surfactants alter the mechanics of interfaces and, as such, their presence can have a profound effect on the macroscale behavior of drops.[8] For instance, it is well known that the free rise/fall of drops can be significantly hindered by the presence of surfactants in the bulk phase. Surfactants adsorbed onto the interface near the leading end of the drop are convected towards its trailing end, where they desorb from the interface and diffuse away through the bulk phase. In this process, a nonuniform surfactant concentration profile is developed on the surface of the drop. If the only effect of surfactant is assumed to be a local reduction in the interfacial tension, the interface will be pulled from the low tension (high surfactant concentration) region at the rear pole to the high tension (low surfactant concentration) region. The resulting tangential (Marangoni) stress resists the surface flow, and eventually causes the interface to behave like a no-slip surface, thereby increasing the drag on the drop and reducing its mobility.

When surface convection is the predominant mechanism for surfactant transport on the interface, and the surfactant flux from the bulk is extremely slow compared to the surface convective flux (i.e., in the limit of an insoluble surfactant monolayer), the interface is partitioned into a surfactant-free region near the leading end of the drop and a surfactant-saturated region near the trailing end which behaves like a stagnant cap. The stagnant cap regime was first examined by Savic,[9] and has since been the subject of several other studies.[10–16] With the exception of the analysis of He *et al.*,[16] all of these studies assumed a linear dependence of the interfacial tension on surfactant concentration. He *et al.*[16] used the (nonlinear) Langmuir adsorption framework to show that

a)Author to whom correspondence should be addressed.

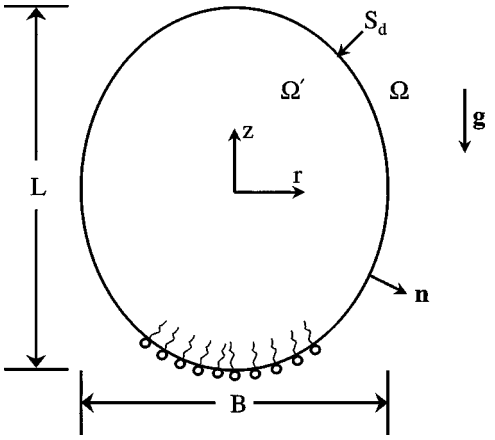

FIG. 1. Definition sketch of a viscous droplet suspended in an otherwise quiescent immiscible fluid of infinite extent.

the linear equation of state underestimates the size of the stagnant cap in the limit of sorption-controlled mass transfer for which the bulk-phase diffusive flux is much faster than the sorptive flux at the interface.

In contrast to the insoluble surfactant limit, the surface concentration varies smoothly over the entire interface when the surfactant flux from the bulk is comparable to the surface convective flux. The induced Marangoni stresses then lead to uniform retardation of the surface velocity over the entire interface. This limit was first studied by Levich[17] who found the reduction in the terminal velocity of a spherical drop whose interfacial tension is slightly perturbed from its equilibrium value. The uniform retardation regime has also been examined by other investigators for trace quantities of surfactants in the diffusion-controlled[18–20] and sorption-controlled[20] mass transfer limits, using a linear adsorption framework. Most recently, Chen and Stebe[21] analyzed the effect of surfactants on drop mobility in the limit of high surface coverage with sorption-controlled mass transfer. Using the Langmuir and Frumkin adsorption frameworks, they showed that the linear framework fails at elevated surface concentrations due to its inability to account for the finite size of adsorbed surfactant molecules and the nonideal interactions among them.

All of the aforementioned studies of the effect of surfactants on the buoyancy-driven motion of drops have focused on the drop mobility, assuming a fixed spherical shape for the drop. In this study, we examine the influence of surfactants on the *stability* of the shape of an axisymmetric drop translating in an unbounded fluid at zero Reynolds number. The Frumkin adsorption framework will be adopted to study surfactant effects at elevated surface concentrations, and both bulk-insoluble and soluble surfactants will be considered.

II. PROBLEM FORMULATION

A. Fluid dynamics

Consider the buoyancy-driven motion of a drop of density $\gamma\rho$ in a large reservoir of an otherwise quiescent fluid of density ρ (see Fig. 1). Since the drop shape is unknown *a priori*, the drop size is characterized by the radius, R, of a spherical drop with equal volume. The exterior and interior bulk phases (denoted by Ω and Ω', respectively) are incompressible and Newtonian with viscosities μ and $\lambda\mu$, respectively, and the entire system is assumed to be isothermal. The two-phase interface, S_d, is described by an interfacial stress tensor that consists of only an isotropic (interfacial) tension, σ. In what follows, all lengths are made dimensionless with R, all velocities with the characteristic velocity $U_b=(1-\gamma)\rho g R^2/\mu$, all stresses with $\mu U_b/R$, and time with R/U_b. The interfacial tension, σ, is made dimensionless by its reference value, σ_{eq}, corresponding to an interface with uniform distribution of surfactant in the absence of flow.

In the low Reynolds number limit, the bulk flow in each phase is governed by the continuity and Stokes equations given by

$$\boldsymbol{\nabla}\cdot\mathbf{u}=0; \quad \boldsymbol{\nabla}p=\nabla^2\mathbf{u}, \quad \text{for } \mathbf{x}\in\Omega, \tag{2}$$

$$\boldsymbol{\nabla}\cdot\mathbf{u}'=0; \quad \boldsymbol{\nabla}p'=\lambda\nabla^2\mathbf{u}' \quad \text{for } \mathbf{x}\in\Omega', \tag{3}$$

where $\mathbf{u}$ and p represent the velocity and the modified pressure, respectively, and all drop phase quantities are denoted by a prime. The dimensionless boundary conditions can be written as

$$(\mathbf{u},p)\rightarrow(-\mathbf{u},0), \quad \text{as } |\mathbf{x}|\rightarrow\infty, \tag{4}$$

$$\mathbf{u}(\mathbf{x})=\mathbf{u}'(\mathbf{x}), \quad \text{for } \mathbf{x}\in S_d, \tag{5}$$

$$\mathbf{n}\cdot\mathbf{u}'(x)=\mathbf{n}\cdot\frac{d\mathbf{x}}{dt}, \quad \text{for } \mathbf{x}\in S_d, \tag{6}$$

$$\mathbf{n}\cdot(\boldsymbol{\Pi}'-\boldsymbol{\Pi})=\frac{1}{\mathrm{Bo}}\left[\left(\frac{d\sigma}{d\Gamma}\right)\boldsymbol{\nabla}_s\Gamma-\sigma\mathbf{n}(\boldsymbol{\nabla}_s\cdot\mathbf{n})-\mathrm{Bo}\,\mathbf{n}(\mathbf{e}_z\cdot\mathbf{x})\right], \quad \text{for } \mathbf{x}\in S_d, \tag{7}$$

where $\boldsymbol{\Pi}$ is the Newtonian stress tensor, $\mathbf{e}_z$ is the unit vector in the axial direction, $\mathbf{n}$ is the unit normal vector on the surface of the drop directed into Ω, and $\boldsymbol{\nabla}_s=(\mathbf{I}-\mathbf{nn})\cdot\boldsymbol{\nabla}$ is the surface gradient operator acting in the plane tangent to the interface. The Bond number, $\mathrm{Bo}=\mu U_b/\sigma_{\mathrm{eq}}$, is defined based on the equilibrium value of the interfacial tension, and represents the ratio of gravitational forces tending to deform the drop to interfacial tension forces resisting deformation. The boundary conditions on the surface of the drop include the continuity of velocity across the interface [Eq. (5)], the kinematic condition [Eq. (6)], and the jump in the interfacial traction vector due to interfacial tension gradients and surface curvature [Eq. (7)].

The first term on the right hand side of Eq. (7) represents the variations of interfacial tension due to gradients in the surface concentration, Γ, of any surface-active molecules adsorbed on the interface, where $d\sigma/d\Gamma$ is given by an appropriate surface equation of state, $\sigma=\sigma(\Gamma)$, as shown in Sec. II C. In the absence of surfactants, there will not be any interfacial tension gradients, and the above set of equations represents a well-posed problem. In the presence of surfac-

tants, these equations must be complemented with the appropriate equations governing the surface concentration of surfactant.

B. Surfactant transport

In the absence of bulk fluid motion, surfactant molecules are free to adsorb and diffuse along the interface, and will establish a uniform concentration, Γ_{eq}, which will be in equilibrium with a bulk concentration, C_{eq}. The interfacial forces that result from bulk fluid motion will tend to disturb this state of equilibrium, and a new balance between surface convection and the competing fluxes due to diffusion and adsorption/desorption will lead to a redistribution of surfactant molecules on the interface, represented by a nonequilibrium surface concentration, Γ (made dimensionless with the maximum concentration for monolayer adsorption Γ_∞). This quantity can also be thought of as a dimensionless surface coverage or saturation since it can never exceed unity. The governing equation for the surface concentration is an unsteady convective-diffusion equation which, in dimensionless form, can be written as[22,23]

$$\frac{\partial \Gamma}{\partial t} + \boldsymbol{\nabla}_s \cdot (\Gamma \mathbf{u}_s) - \frac{1}{\mathrm{Pe}_s} \boldsymbol{\nabla}_s^2 \Gamma + \Gamma H(\mathbf{u}\cdot\mathbf{n}) = -\mathbf{n}\cdot\mathbf{q}, \quad \text{for } \mathbf{x} \in S_d, \tag{8}$$

where $\mathbf{u}_s = (\mathbf{I}-\mathbf{nn})\cdot\mathbf{u}$ is the surface velocity vector, the surfactant flux, $\mathbf{q}$, is made dimensionless with $U_b\Gamma_\infty/R$, and the surface Peclet number $\mathrm{Pe}_s = U_b R/\mathcal{D}_s$ represents the relative importance of the convective to diffusive transport of surfactant on the interface, with $\mathcal{D}_s$ being the surface diffusivity of surfactant. The first three terms on the LHS of Eq. (8) represent the conventional accumulation, convection, and diffusion of surfactant, while the last term accounts for the variations in surfactant concentration resulting from local stretching and deformation of the interface. The term on the RHS of Eq. (8) represents the dimensionless rate at which surfactant is supplied from the bulk to the interface.

The surfactant is assumed to be soluble only in the suspending fluid phase (and not in the drop phase). Furthermore, convective transport of surfactant in the suspending fluid is assumed to be negligible so that surfactant transport between the interface and the bulk occurs through a combination of kinetic adsorption/desorption and molecular diffusion. The latter assumption leads to a linear surfactant transport problem in the suspending fluid, and is strictly valid only in the limit of a small bulk-phase Peclet number (defined as $\mathrm{Pe} = U_b R/\mathcal{D}$, where $\mathcal{D}$ is the bulk diffusivity of surfactant). Physically, this approximation implies a small diffusive time scale, as in the case of a surfactant with a large bulk-phase diffusivity. The bulk-phase surfactant concentration C (made dimensionless with C_{eq}) is thus governed by Laplace's equation,

$$\nabla^2 C = 0, \quad \text{for } \mathbf{x} \in \Omega. \tag{9}$$

This equation is solved subject to the Dirichlet condition that the surfactant concentration decays to its equilibrium value far from the drop,

$$C = 1, \quad \text{for } |\mathbf{x}| \to \infty, \tag{10}$$

and the interface flux condition

$$\mathbf{n}\cdot\nabla C = -\epsilon \mathrm{Pe}(\mathbf{n}\cdot\mathbf{q}), \quad \text{for } \mathbf{x} \in S_d, \tag{11}$$

where $\epsilon = \Gamma_\infty / C_{eq} R$ is a measure of the thickness of the surfactant depletion sublayer adjacent to the interface. The latter condition is obtained by requiring the diffusive flux of surfactant from the bulk to the sublayer to be equal to the net adsorptive flux of surfactant at the interface. Assuming the adsorption rate to be first order in both the bulk surfactant concentration at the interface and the available space on the interface (analogous to second-order adsorption kinetics), and the desorption rate to be first order in the surface concentration Γ, the net adsorptive flux can be written in dimensionless form as

$$-\mathbf{n}\cdot\mathbf{q} = \mathrm{Bi}[KC(1-\Gamma) - \Gamma], \tag{12}$$

where Bi is a Biot number, representing the ratio of the characteristic sorption rate to the rate of interfacial convection of surfactant, and K is the equilibrium surfactant partition coefficient, representing the ratio of the characteristic adsorption to desorption rate at the interface. Using Eq. (12), the interface flux condition [Eq. (11)] can be rewritten as

$$\mathbf{n}\cdot\nabla C = \mathrm{Da}[KC(1-\Gamma) - \Gamma], \tag{13}$$

where $\mathrm{Da} = \epsilon\,\mathrm{Pe}\,\mathrm{Bi}$ is a Damkohler number, representing the ratio of the characteristic adsorptive to diffusive flux.

Depending on the value of the Damkohler number, several mass transfer regimes can be identified for nonzero values of Bi. For small values of Da, the adsorption/desorption process between the sublayer and the interface is much slower than bulk-phase diffusion, and surfactant mass transfer is *sorption-controlled*. In this regime, a uniform bulk concentration $C \simeq 1$ is maintained everywhere in the suspending fluid. On the other hand, for large values of Da, surfactant diffusion from the bulk to the sublayer is much slower than the adsorption/desorption process, and surfactant mass transfer is *diffusion-controlled*. In this regime, equilibrium between the sublayer and the interface is essentially established instantaneously, and the surfactant is partitioned between them according to an equilibrium adsorption isotherm (as described in the next section). In the limit $\mathrm{Da} \to \infty$, the flux of surfactant from the bulk to the sublayer tends to zero and the mass transfer problem approaches that for an insoluble surfactant.

C. Surfactant thermodynamics

Before a solution to the transport equations can be obtained, a surface equation of state describing the dependence of interfacial tension σ on surfactant concentration Γ must be specified. The first step is the selection of an adsorption framework. The Frumkin adsorption framework, which is most appropriate for nonionic surfactants, will be used in this study. The Frumkin adsorption isotherm is a lattice-type model that accounts for both the finite size of surfactant molecules and the nonideal interactions among them. In dimensionless form, it can be written as (cf. Chang and Franses[24])

$$\Gamma = \frac{KC}{KC + \exp(\xi\Gamma)}, \tag{14}$$

where the surface concentration Γ is made dimensionless with the maximum surface concentration for monolayer adsorption, Γ_∞, and the interaction parameter ξ is a measure of the nonideality of mixing at the interface. The surface saturation concentration Γ_∞ is a theoretical limit that is important, but normally will not be reached due to constraints on the maximum bulk concentration such as the critical micelle concentration or the solubility. The interaction parameter ξ is negative for cohesive interactions and positive for repulsive interactions. When the interaction parameter becomes zero, the Frumkin isotherm reduces to the Langmuir isotherm. An important feature of the Frumkin and Langmuir isotherms is their ability to account for surface saturation effects, i.e., the dimensional surface concentration cannot exceed the surface saturation concentration Γ_∞.

The appropriate surface equation of state corresponding to the selected adsorption framework is dictated by interfacial thermodynamics. The dimensionless Gibbs adsorption equation at constant temperature is

$$d\sigma = -E\Gamma d(\ln C), \tag{15}$$

where the elasticity number $E = RT\Gamma_\infty/\sigma_{\mathrm{eq}}$ is a measure of the sensitivity of interfacial tension to variations in surfactant concentration. Integration of Eq. (15) using the Frumkin adsorption isotherm leads to the following surface equation of state:

$$\sigma = \sigma_c + E\left[\ln(1-\Gamma) - \frac{1}{2}\xi\Gamma^2\right], \tag{16}$$

where σ_c is the interfacial tension of the clean interface made dimensionless with σ_{eq}. The interfacial tension distribution on the surface of the drop is then determined by assuming the surface equation of state to apply locally for nonuniform surfactant distributions. It should be noted that σ_c and K are not independent parameters, and can be calculated from the equation of state and the adsorption isotherm, respectively, according to

$$\sigma_c = 1 - E\left[\ln(1-\Gamma_{\mathrm{eq}}) - \frac{1}{2}\xi\Gamma_{\mathrm{eq}}^2\right] \tag{17}$$

and

$$K = \frac{\Gamma_{\mathrm{eq}}\exp(\xi\Gamma_{\mathrm{eq}})}{1-\Gamma_{\mathrm{eq}}}. \tag{18}$$

In the dilute limit $\Gamma_{\mathrm{eq}} \ll 1$, Eq. (16) reduces to the more commonly used linear equation of state. Because of its inability to capture surface saturation effects that will be present at elevated surfactant concentrations, the linear equation of state overpredicts the reduction in interfacial tension at high surface coverages. Hence, it is strictly valid only in the limit of very dilute surfactant concentrations.

Nonlinear effects can have a significant impact on the interfacial tension distribution. This is most clearly visualized by plotting the isotherms for different types of surfactants in the form of nondimensional surface pressure, defined as $\Pi = (\sigma_c - \sigma)/E$, versus dimensionless surface coverage (shown in Fig. 2). Physically, surface pressure represents the work per unit area required to compress the monolayer to add more surfactant to the interface. Thus, the surface pressure is nearly zero for low surface coverages encountered in the dilute limit, while it diverges for surface coverages approaching monolayer saturation. For any surface coverage, it is more difficult to add surfactant to the interface in the presence of repulsive molecular interactions, compared to the ideal case of a Langmuir surfactant with no molecular interactions, i.e., the surface pressure for positive ξ is larger than that for $\xi = 0$ at any value of Γ. On the other hand, surfactants which exhibit cohesive interactions (negative ξ) require less energy to be added to the interface, and hence lead to smaller surface pressures, than Langmuir surfactants. For $\xi = -4$, corresponding to surfactants with strong cohesive interactions, close inspection of Eq. (16) reveals that the surface pressure has a critical point at 50% surface coverage, such that any stronger cohesion would result in a surface phase change (cf. Ferri and Stebe[25]). The existence of an inflection point is also demonstrated by the plateau in the surface pressure isotherm for such a surfactant (shown in Fig. 2). This plateau can be thought of as a coexistence region between a surface expanded state at low surface saturation and a surface condensed (or aggregated) state at high surface saturation, where surface pressure becomes essentially independent of surface coverage.

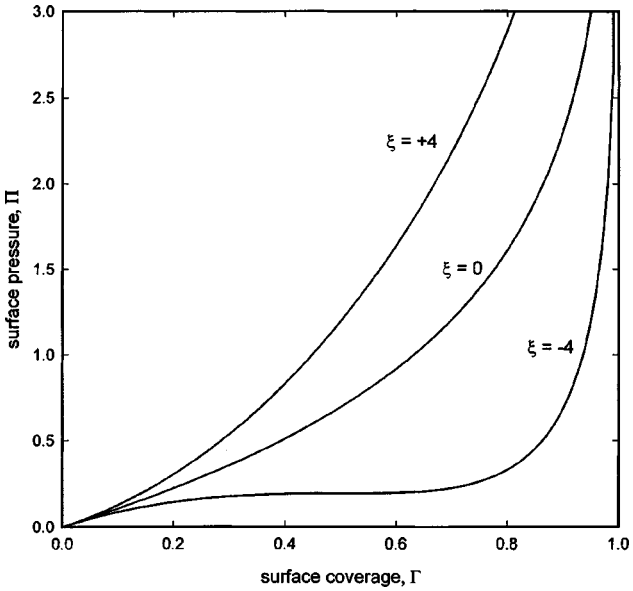

FIG. 2. The dependence of surface pressure on surface coverage based on the Frumkin model for surfactants with cohesive interactions (negative ξ), repulsive interactions (positive ξ), and no interactions (i.e., the Langmuir model).

III. SOLUTION PROCEDURE

In the absence of inertial and convective effects in the fluid dynamics and bulk surfactant transport problems, respectively, the governing equations [Eqs. (2), (3), and (9)] are linear, and the boundary integral method provides a convenient and efficient means of solving for the bulk surfactant concentration and the flow field. Following the standard boundary integral formulation of the Stokes and Laplace

equations, and using boundary conditions (7) and (13), integral equations for the interfacial velocity and the sublayer concentration distributions can be written as

$$\mathbf{u}(\mathbf{x}_0)=\frac{2}{\mathrm{Bo}(1+\lambda)}\int_{S_d}\mathbf{J}\cdot\left[\left(\frac{d\sigma}{d\Gamma}\right)\nabla_s\Gamma-\sigma\mathbf{n}(\nabla_s\cdot\mathbf{n})-\mathrm{Bo}\,\mathbf{n}(\mathbf{x}\cdot\mathbf{e}_z)\right]dS(\mathbf{x})+\frac{2(1-\lambda)}{(1+\lambda)}\int_{S_d}\mathbf{K}\cdot\mathbf{u}\cdot\mathbf{n}\,dS(\mathbf{x}),\tag{19}$$

$$\hat{C}(\mathbf{x}_0)=-2\int_{S_d}\{\hat{C}\mathbf{n}\cdot\mathbf{K}_c+J_c\,\mathrm{Da}[K(1-\hat{C})(1-\Gamma(\mathbf{x}))-\Gamma(\mathbf{x})]\}dS(\mathbf{x}),\tag{20}$$

where $\hat{C}=1-C$ is the disturbance bulk concentration, $\mathbf{x}$ is the integration variable, and $\mathbf{x}_0$ is a fixed point on the interface. The fundamental solutions of the Stokes and Laplace equations appearing in these expressions are given by

$$\mathbf{K}=-\frac{3}{4\pi}\left(\frac{\hat{\mathbf{x}}\hat{\mathbf{x}}\hat{\mathbf{x}}}{r^5}\right),\tag{21}$$

$$\mathbf{J}=\frac{1}{8\pi}\left(\frac{\mathbf{I}}{r}+\frac{\hat{\mathbf{x}}\hat{\mathbf{x}}}{r^3}\right),\tag{22}$$

$$\mathbf{K}_c=-\frac{1}{4\pi}\left(\frac{\hat{\mathbf{x}}}{r^3}\right),\tag{23}$$

$$J_c=\frac{1}{4\pi r},\tag{24}$$

where $\hat{\mathbf{x}}=\mathbf{x}_0-\mathbf{x}$ and $r=|\hat{\mathbf{x}}|$.

The coupled system of equations formed by the fluid dynamics and surfactant transport problems were solved in an iterative manner. A standard boundary collocation technique was used to solve Eqs. (19) and (20) for the interfacial velocity and sublayer concentration distributions, while a Crank–Nicholson time-marching scheme along with a second-order accurate finite-difference approximation [on the same grid as that used in the solution of Eqs. (19) and (20)] was used to solve the surface convective-diffusion equation [Eq. (8)]. Since only axisymmetric drop deformations were considered, the surface integrals in Eqs. (19) and (20) were reduced to line integrals by performing the azimuthal integrations analytically. The line integrals were then evaluated numerically using a combination of an iterated Romberg method and Gauss–Legendre quadrature with quadratic variations of $\mathbf{u}$ and $\hat{C}$ over each element on the interface. Details of the integration procedure are provided elsewhere.[26]

In order to study the stability of a spherical drop to finite perturbations in drop shape, the computations were initiated with either an oblate or a prolate ellipsoidal drop shape. Following Koh and Leal,[4] the initial shape perturbation was characterized by the deformation parameter $\Delta=(L-B)/(L+B)$ (where L and B are defined in Fig. 1), so that negative and positive values of Δ correspond to oblate and prolate initial deformations, respectively. A uniform surfactant distribution corresponding to the equilibrium surface coverage $\Gamma=\Gamma_{\mathrm{eq}}$ was used as the initial condition for the surfactant concentration on the surface of the drop. Starting with the initial shape and surfactant concentration profile, the boundary integral equations were solved for the unknown surface velocity and sublayer concentration distributions. Subsequently, the kinematic condition [Eq. (6)] was integrated using an explicit Euler method to update the drop shape, and a new surfactant distribution on the surface of the drop was obtained by solving the surface convective-diffusion equation. After each time step, the collocation points were redistributed over the new interface to maintain elements of equal size, and the drop volume was calculated to estimate the truncation error. The iterations were carried out until either steady-state was achieved or the drop appeared to be on the verge of breakup. Typically 40 elements were used to discretize the surface of the drop, but this number was increased in the case of highly deformed drops with regions of large curvature. All computations were performed on IBM RS/6000 workstations.

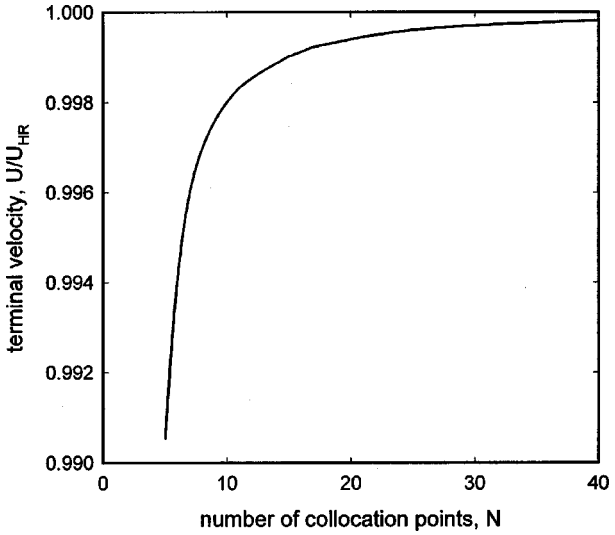

FIG. 3. the steady migration velocity (scaled by the Hadamard–Rybzynski velocity, U_{HR}) as a function of the number of collocation points, N, on the surface of the drop.

IV. RESULTS AND DISCUSSION

In order to check the accuracy of the numerical scheme, we compared the computed velocity of a spherical drop with the corresponding prediction based on the Hadamard–Rybzynski solution [given by Eq. (1)]. Figure 3 shows the computed terminal velocity of a drop with $\lambda=1$ as a function of the number of collocation points used in the computations. Clearly, for $N\geqslant 40$, the computations converge to the exact solution to within at least 0.05%. We also performed mesh refinement studies to ensure sufficient resolution to reproduce the computational results of Koh and Leal,[4] and Pozrikidis,[6] for the evolution of the shape of clean drops. For all of the computations reported in this section, the values of the viscosity ratio and the elasticity number were fixed at $\lambda=1$ and $E=0.4$, respectively.

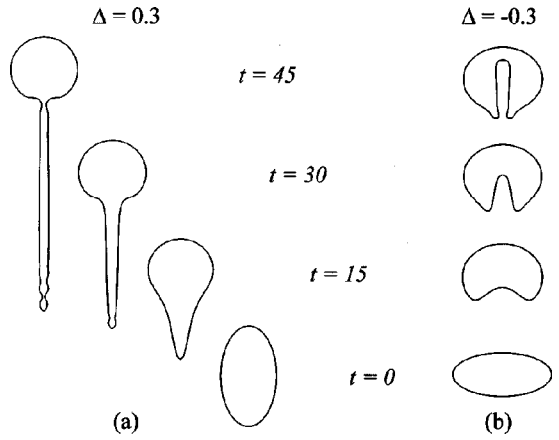

FIG. 4. The time-evolution of the shape of an initially ellipsoidal drop with Bo=25 in the absence of surfactants; (a) $\Delta=0.3$, (b) $\Delta=-0.3$.

For sufficiently small Bond numbers, clean drops that are initially perturbed into an ellipsoidal shape (either prolate or oblate) revert to a spherical shape. For Bond numbers beyond a critical value, however, initially perturbed drop shapes continuously deform until drop breakup occurs through one of the two mechanisms described by Koh and Leal,[4] and Pozrikidis,[6] depending on the nature of the initial shape perturbation. In the case of initially-prolate drop shapes (i.e., for positive values of Δ), drop breakup occurs through the formation of a tail at the trailing end of the drop, which continuously elongates in time and eventually pinches off either at a single point near the main body of the drop or at multiple points along the tail due to the development of finite amplitude capillary wave instabilities [see Fig. 4(a)]. For initially-oblate drop shapes (i.e., for negative values of Δ), the breakup mechanism consists of the formation and growth of a re-entrant cavity at the trailing end of the drop [see Fig. 4(b)], which either collapses at the trailing end of the drop to form a separate drop of suspending fluid within the original drop, or completely penetrates through the drop to form a torus, similar to the behavior reported by Kojima *et al.*[3] for drops with zero interfacial tension ($\mathrm{Bo}\rightarrow\infty$). At this point, it should be emphasized that the evolution of the drop shape could not be computed accurately near the point of actual pinch-off. Computations were carried out until the dimensionless thickness of any neck regions became smaller than a predetermined limit [typically $O(10^{-3})$], at which point drop breakup was considered to be imminent.

The stability behavior of a surfactant-laden translating drop is qualitatively similar to that of a clean drop in that, for any initial shape perturbation, there exists a critical value of the Bond number beyond which the drop becomes unstable. In contrast to the case of clean drops, however, stable drops in the presence of surfactants do not attain a spherical shape. This is demonstrated by the variations in surface curvature of the steady drop shapes shown in Fig. 5(a) as a function of the normalized arclength s', where $s'=0$ and $s'=1$ represent the front and rear stagnation points on the drop profile, respectively. The interfacial tension variation created across the surface of the drop by the nonuniform surface distribution of surfactants leads to a slightly oblate steady drop

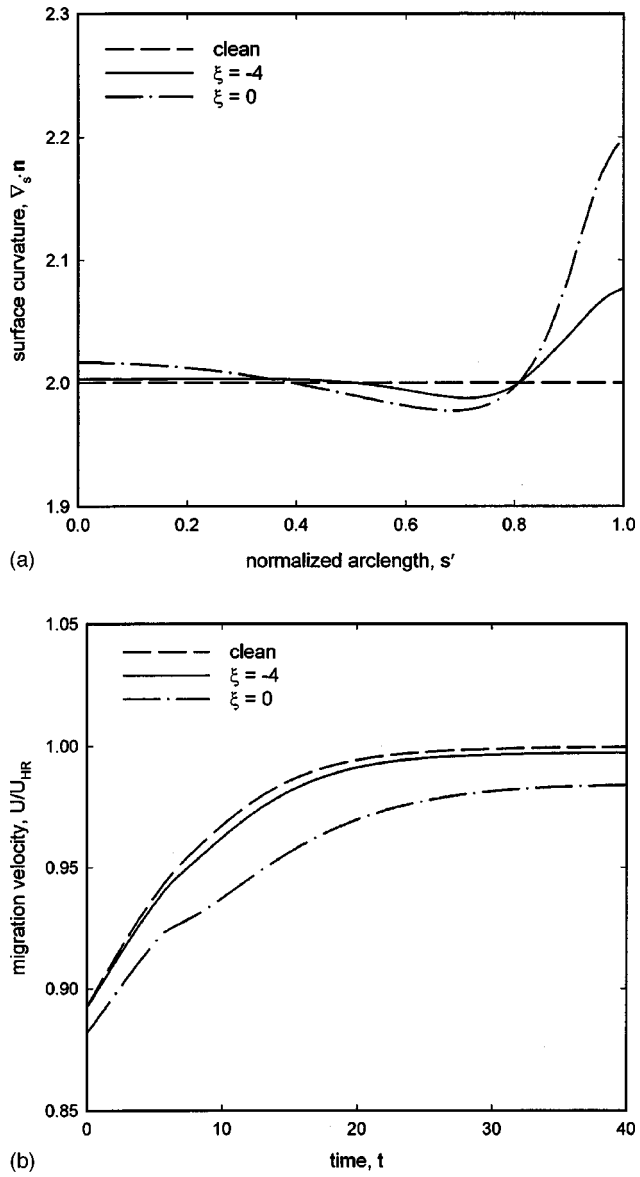

FIG. 5. The steady-state surface curvature distribution (a) and the time-evolution of the migration velocity (b) for stable surfactant-laden drops with $\mathrm{Bo}_c=6.0$, $\Delta=-0.3$, and $\mathrm{Pe}_s=10$.

shape in the presence of surfactants. The associated Marangoni stresses at the interface retard the motion of the drop as a whole, as evidenced by the time-evolution of the migration velocity of the drop shown in Fig. 5(b). The increase in surface curvature at the rear stagnation point of the drop and the reduction in its migration velocity become more pronounced as the cohesive interactions between surface molecules become weaker, due to the larger interfacial tension variations induced across the surface of the drop. Unstable drops in the presence of surfactants eventually break up through one of the mechanisms described by Koh and Leal,[4] and Pozrikidis,[6] for the breakup of clean drops. The difference in the stability behavior of clean and surfactant-laden drops lies in the critical conditions for the onset of drop breakup, which are strongly affected by the time-evolution of the interfacial tension distribution on the surface of the drop, as will be discussed in the following sections.

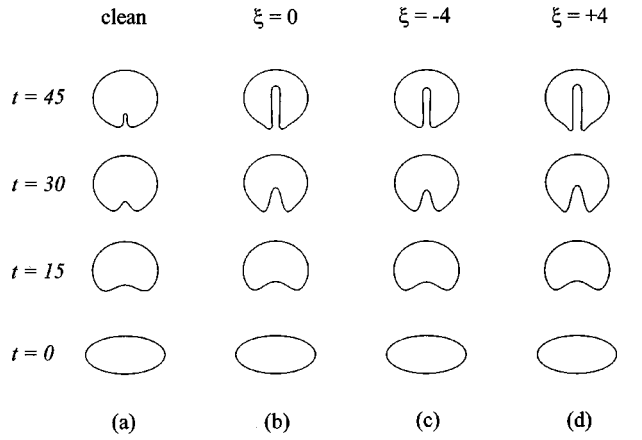

FIG. 6. The time-evolution of the shape of an initially-oblate drop with $\Delta = -0.3$ and $Pe_s = 10$; (a) clean drop with $Bo_c = 12.0$, (b) Langmuir surfactant ($\xi = 0$) with $Bo_c = 12.0$ (Bo=15.3), (c) strongly-cohesive surfactant with $\xi = -4$ and Bo=15.3, (d) strongly-repulsive surfactant with $\xi = +4$ and Bo=15.3.

A. Insoluble surfactants

In this section, the effect of bulk-insoluble surfactants on the critical conditions for the onset of drop breakup is investigated. In order to probe the effects of a surface phase change in the case of strongly-cohesive surfactants, the equilibrium surface coverage is fixed at $\Gamma_{eq} = 0.5$ which corresponds to the critical point of the surface pressure isotherm for surfactants with $\xi = -4$. Consider first the case of a drop with $\Delta = -0.3$ which corresponds to an initially oblate drop shape. The nonlinear evolution of the drop shape is shown in Fig. 6 for clean and surfactant-laden drops. In order to show the effect of surfactants on drop deformation, the behavior of the clean drop is compared to that of a surfactant-laden drop with the same value of Bo_c [see Figs. 6(a) and 6(b)], where Bo_c represents the Bond number based on the interfacial tension of the clean interface. The behavior of surfactant-laden drops in Fig. 6 is presented at a fixed value of the Bond number Bo (based on the equilibrium value of the interfacial tension) to identify the effect of nonideal interactions among surfactant molecules on drop deformation. The drop shapes are shown at equal intervals of 15 dimensionless time units. While all four drops break up through the formation of a re-entrant cavity at the rear stagnation point of the drop, it is clear that the surfactant-laden drops are less stable than the clean drop in the sense that the cavity grows at a faster rate in the presence of surfactants. Furthermore, surfactant-laden drops become more unstable with increasing values of ξ (i.e., as the cohesive interactions among surfactant molecules are weakened). A better understanding of the drop breakup mechanism can be obtained by examining the surface distributions of surfactant and interfacial tension.

The interfacial velocity profiles corresponding to the drop shapes at $t = 30$ in Fig. 6 are shown in Fig. 7(a). The tangential component of velocity in a drop-fixed reference frame is plotted as a function of the arclength s, where $s = 0$ corresponds to the front stagnation point of the drop. Clearly, the presence of surfactants leads to a reduction in the interface mobility over the convex portion of the drop

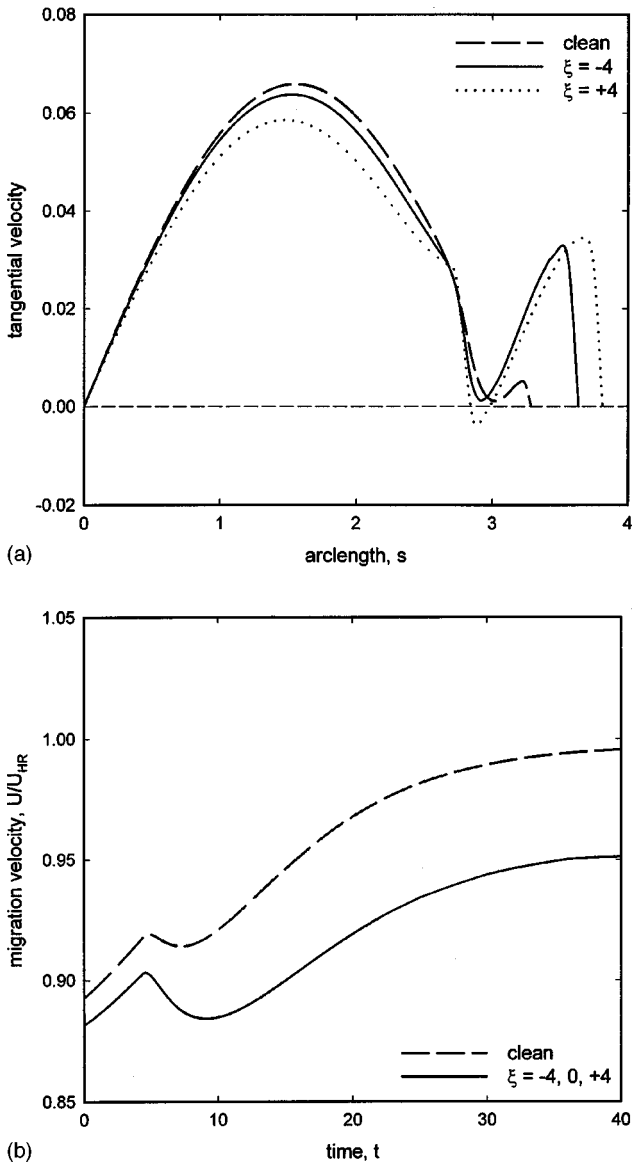

FIG. 7. The surface velocity profile (a) and the time-evolution of the migration velocity (b) for drops shown in Fig. 6 at $t = 30$.

surface, accompanied by a simultaneous increase in interfacial velocity over the part of the drop surface comprising the re-entrant cavity. The latter effect is consistent with the faster growth rate observed for the cavity in the presence of surfactants. A comparison of the two surfactant-laden drops in Fig. 7(a) reveals that the deviations from the clean interface behavior are more pronounced for the strongly-repulsive surfactant. For $\xi = +4$, the interface mobility is reduced to such an extent that stagnation rings develop in the high curvature region at the entrance of the re-entrant cavity. The overall reduction in the migration velocity of the drop due to the presence of surfactants is about the same for all three surfactants considered, as shown by the time-evolution of the rise velocities in Fig. 7(b).

The surface coverage and interfacial tension distributions corresponding to the drop shapes at $t = 30$ in Fig. 6 are shown in Fig. 8 as a function of the normalized arclength. In general, surfactants are accumulated near the trailing end of

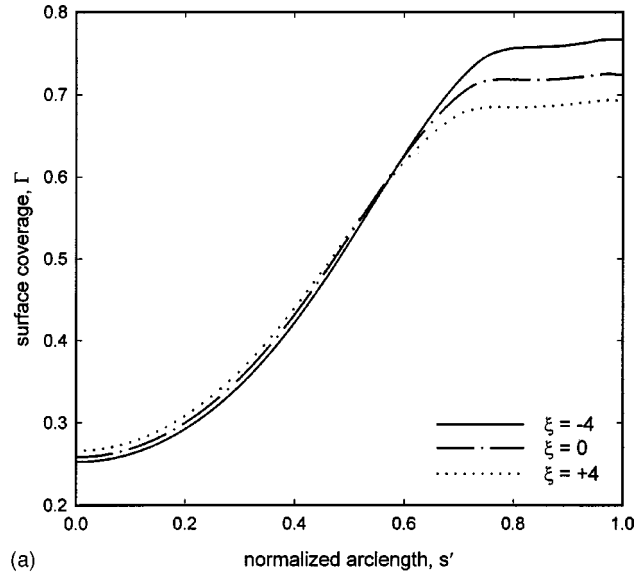

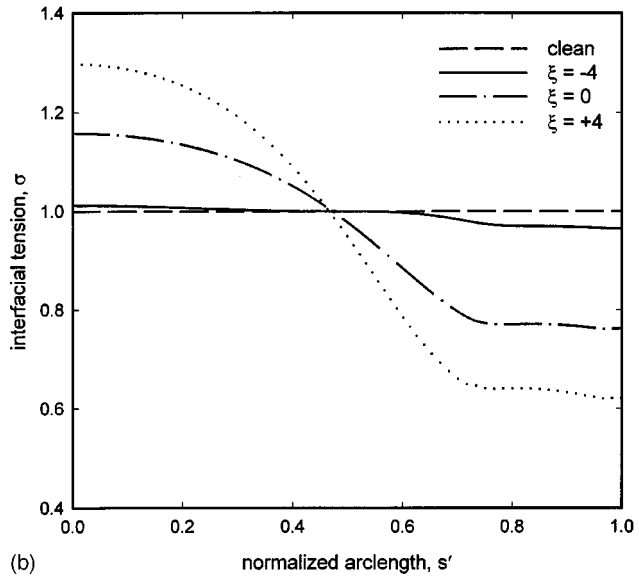

FIG. 8. The surface coverage (a) and interfacial tension (b) distributions for drops shown in Fig. 6 at $t=30$.

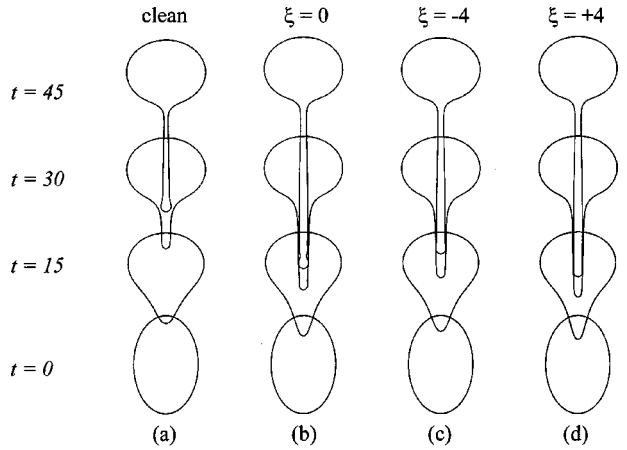

FIG. 9. The time-evolution of the shape of an initially-prolate drop with $\Delta=0.3$ and $\mathrm{Pe}_s=10$; (a) clean drop with $\mathrm{Bo}_c=7.0$, (b) Langmuir surfactant ($\xi=0$) with $\mathrm{Bo}_c=7.0$ (Bo=8.9), (c) strongly-cohesive surfactant with $\xi=-4$ and Bo=8.9, (d) strongly-repulsive surfactant with $\xi=+4$ and Bo=8.9.

the drop, and depleted at the leading end, relative to the equilibrium surface coverage of $\Gamma_{\mathrm{eq}}=0.5$. Even though surfactant accumulation on the portion of the interface within the cavity is larger for the strongly-cohesive surfactant [see Fig. 8(a)], Fig. 8(b) shows that the interfacial tension in the unstable cavity is actually lower for the Langmuir and strongly-repulsive surfactants. This counter-intuitive relation between surfactant concentration and interfacial tension can be understood by referring to the surface pressure-surface coverage isotherm shown in Fig. 2. For any given surface coverage, the surface pressure is larger (i.e., the interfacial tension is smaller) for surfactants with weaker cohesive interactions since it is energetically ''easier'' to pack surfactants with cohesive molecular interactions on the interface. The lower interfacial tension in the cavity for the strongly-repulsive surfactant (relative to the strongly-cohesive surfactant) requires larger interfacial deformations in that region to satisfy the normal stress balance. This is a destabilizing effect in that the region of the interface with lowered isotropic tension will reach the critical conditions for drop breakup at a lower Bond number.

We now examine the shape evolution of initially-prolate drop shapes with $\Delta=0.3$, as shown in Fig. 9. Once again, the destabilizing effect of surfactants is evident from a comparison of the shapes of clean drops and surfactant-laden drops with $\xi=0$ at a fixed value of Bo_c. In particular, the unstable tail of surfactant-laden drops forms earlier and grows at a faster rate than the characteristic rate of $(1+\lambda)^{-1}$ predicted by the linear stability analysis of Kojima *et al.*[3] for clean drops. The surfactant-laden drops shown in Fig. 9 are all characterized by the same value of the Bond number based on the equilibrium value of the interfacial tension. The faster growth of the unstable tail of surfactant-laden drops for larger values of ξ indicates that, as in the case of initially-oblate drop shapes, drops are less stable in the presence of surfactants with stronger repulsive interactions. The surface velocity profiles presented in Fig. 10(a) for the drop shapes at $t=30$ in Fig. 9 show trends that are qualitatively similar to those presented in Fig. 7(a) for initially oblate drops. Namely, in the presence of surfactants, the interface mobility is retarded over the main body of the drop, with the reduction in interface velocity being most pronounced in the case of strongly-repulsive surfactants. In the tail region, on the other hand, interface velocities are larger when surfactants are present. Overall, surfactants have a retarding effect on the mobility of the drop as a whole, as demonstrated by the time-evolution of the migration velocities in Fig. 10(b). In contrast to the initially-oblate drops, however, the reduction in the migration velocity of initially-prolate drops is more pronounced for surfactants with stronger repulsive interactions. For the surfactant-laden drops in Fig. 9, surfactant concentration in the tail region is much higher than that over the main body of the drop, with local accumulation of surfactants in the neck region joining the tail and the main body of the drop [see Fig. 11(a)]. As expected, the interfacial tension over the tail region is significantly lower for the strongly-repulsive surfactants compared to that for the strongly-

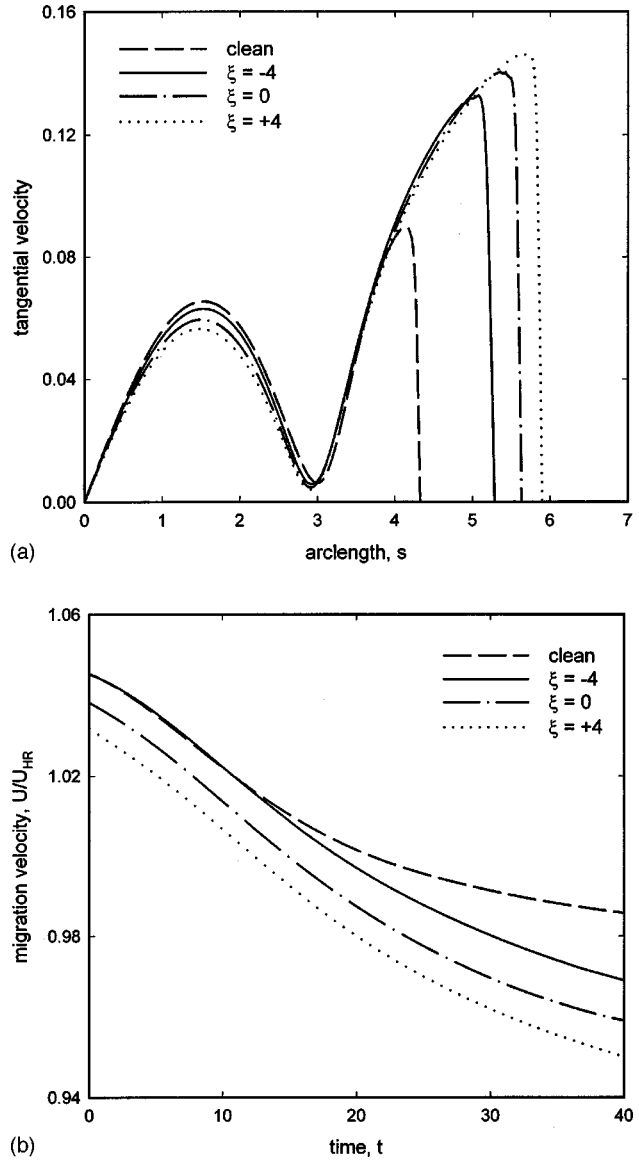

FIG. 10. The surface velocity profile (a) and the time-evolution of the migration velocity (b) for drops shown in Fig. 9 at $t=30$.

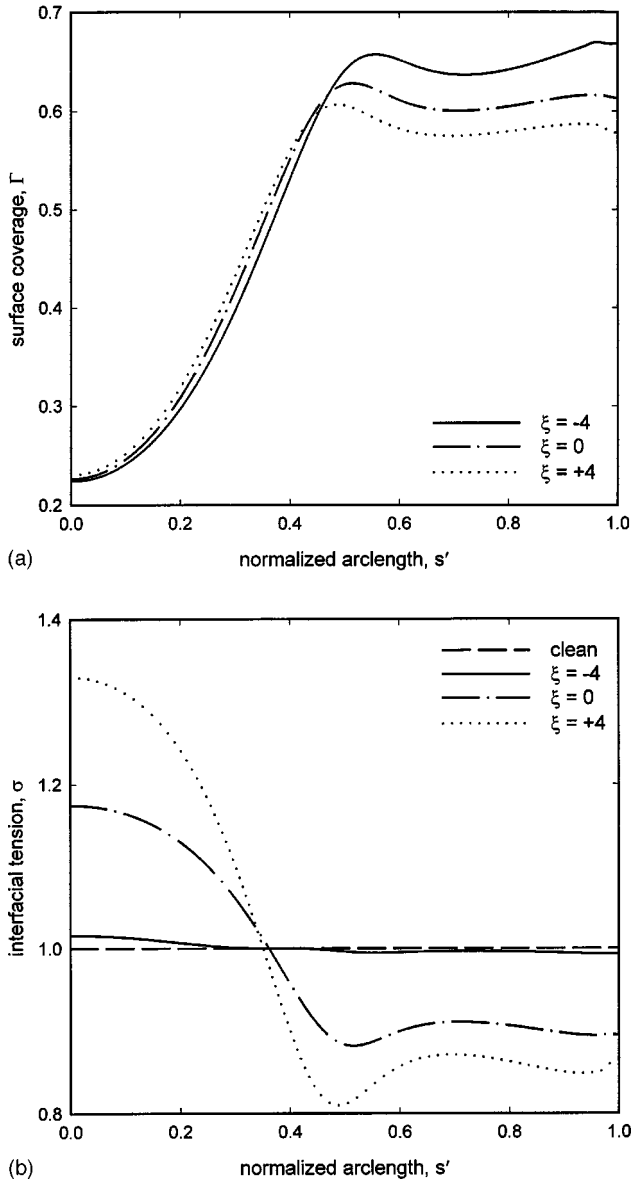

FIG. 11. The surface coverage (a) and interfacial tension (b) distributions for drops shown in Fig. 9 at $t=30$.

cohesive surfactants, and experiences a local minimum in the neck region [see Fig. 11(b)]. This has a destabilizing effect on the shape of the drop by accelerating the formation of the neck.

The presentation of results has heretofore focused on the effect of surfactants on the shape evolution of unstable drops with fixed initial shape perturbation and Bond numbers larger than the critical value for the onset of drop breakup. For clean drops, Koh and Leal[4] showed that the stability of the drop shape depends on both the magnitude of the initial shape perturbation and the Bond number. Specifically, they found that as the extent of initial deformation decreases, the critical Bond number for the onset of breakup increases. In the infinite Bond number (zero interfacial tension) limit, drops are unstable to infinitesimal perturbations from the steady spherical shape, as predicted by the linear stability analysis of Kojima *et al.*[3] The effect of bulk-insoluble surfactants on the critical conditions for drop breakup is shown in Fig. 12 for $\mathrm{Pe}_s=10$. The curves in this figure represent the marginal stability boundaries in the sense that conditions to the left of these curves result in steady drop shapes while those to the right lead to drop breakup through one of the two mechanisms described earlier. Clearly, the trends described earlier for fixed values of $\Delta=\pm 0.3$ hold true for a wide range of initial deformations. Namely, for the same initial deformation (either prolate or oblate), clean drops are more stable than those translating in the presence of surfactants. The effect of surfactants on the critical Bond number becomes much more pronounced as the value of the interaction parameter increases (or, equivalently, as the cohesive interactions among surface molecules are weakened). In fact, the marginal stability curve for surfactants with strongly-cohesive interactions is nearly the same as that for clean drops.

It is interesting to consider the effect of surface Peclet

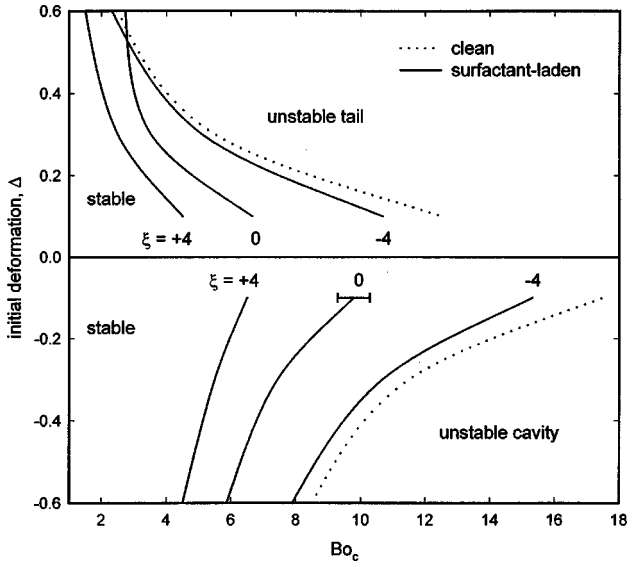

FIG. 12. The marginal stability diagram for drops translating in the presence of bulk-insoluble surfactants at $\mathrm{Pe}_s = 10$.

number on the marginal stability curves. Increasing the surface Peclet number leads to an increase in surfactant accumulation at the trailing end of the drop, accompanied by a reduction in the interfacial tension there, as shown in Fig. 13 for $\xi = -4$ and $\mathrm{Bo} = 2.0$. The collapse of all three curves in Fig. 13(b) to $\sigma = 1$ in the vicinity of $s \simeq 0.5$ is caused by the plateau in the surface pressure isotherm for $\xi = -4$, over which interfacial tension is essentially independent of surfactant concentration. For $\mathrm{Pe}_s = 50$, the trailing end of the drop is almost fully saturated, causing the interfacial tension to drop to about 30% of its equilibrium value. The presence of such dramatic variations in interfacial tension on the surface of the drop leads to nonspherical steady shapes for stable drops, as evidenced by the nonuniform distributions of surface curvature shown in Fig. 13(c). For sufficiently large values of Pe_s, the interfacial tension becomes nearly zero over a cap-like region at the trailing end of the drop. This can have a significant impact on the stability of the drop shape since, as was shown by Kojima *et al.*,[3] drops with zero interfacial tension are unstable to infinitesimal shape perturbations. Hence, it is possible that for sufficiently large values of Pe_s, there is a finite value of $\mathrm{Bo}_{\mathrm{crit}}$ beyond which drops become unstable to infinitesimal perturbations so that no stable drop shapes exist for $\mathrm{Bo} > \mathrm{Bo}_{\mathrm{crit}}$ regardless of the value of Δ. In terms of the marginal stability diagram shown in Fig. 12, this would imply that, for surface Peclet numbers greater than a limiting value, the marginal stability curves for positive and negative values of Δ would intersect each other at a finite value of Bo_c. For clean drops, on the other hand, the marginal stability curves for positive and negative values of Δ asymptotically approach the $\Delta = 0$ axis as the Bond number tends to infinity. Unfortunately, we could not obtain accurate results for surface Peclet numbers much larger than 50 because the surface pressure would diverge at surface coverages approaching unity, thereby leading to negative values of interfacial tension at the trailing end of the drop.

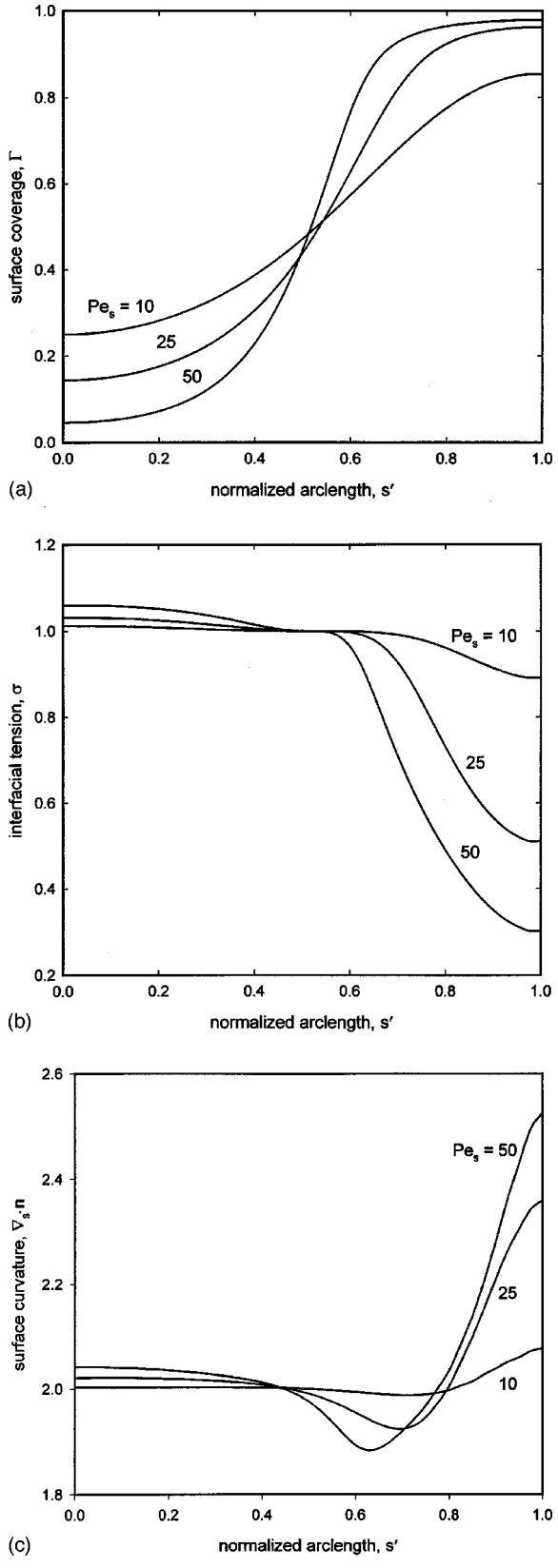

FIG. 13. The steady-state surface coverage (a), interfacial tension (b), and surface curvature (c) distributions for stable surfactant-laden drops with $\mathrm{Bo}_c = 2.0$, and $\xi = -4$.

B. Bulk-soluble surfactants

In this section, the effect of bulk-soluble surfactants on the stability of translating drops is examined, and the results

are compared with those presented in the previous section for bulk-insoluble surfactants. The dimensionless parameters for the bulk-phase surfactant transport problem are fixed at Da $=0.1$ and Bi$=1.0$ so that surfactant mass transfer is neither diffusion-controlled nor sorption-controlled. We first consider the behavior of drops with $\mathrm{Bo}_c < \mathrm{Bo}_{\mathrm{crit}}$, for which a steady drop shape is achieved. The steady-state surface velocity, surfactant concentration, and interfacial tension profiles for drops translating in the presence of a strongly-cohesive surfactant ($\xi = -4$) with $\mathrm{Pe}_s = 50$ are shown in Fig. 14. In the presence of insoluble surfactants, interface mobility is significantly retarded compared to the surfactant-free case, and a stagnant cap region begins to develop at the trailing end of the drop [see Fig. 14(a)]. This result was also predicted by Chen and Stebe[21] for nondeforming drops settling in a surfactant solution. In general, bulk-solubility has the effect of increasing the interfacial velocity to such an extent that the surfactant-free surface velocity profile is retrieved. The surfactant concentration profiles presented in Fig. 14(b) demonstrate that bulk solubility has the effect of restoring a more uniform surface distribution of surfactant, while simultaneously reducing the total amount of surfactant adsorbed at the interface. The amount of surfactant present on the surface of the drop is dictated by the equilibrium partition coefficient, K, which depends on the equilibrium surface coverage and the interaction parameter according to Eq. (18). The value of the partition coefficient corresponding to the parameter values in Fig. 14 (i.e., for 50% equilibrium surface coverage of a strongly-cohesive surfactant with $\xi = -4$) is $K = 0.135$, indicating the rate of surfactant desorption to be larger than that of adsorption. Thus, compared to the insoluble surfactant case, surfactant is ''bled'' from the interface to the bulk. The resulting bulk concentration profile at the interface follows the general trend of the surface coverage profile, though its variations around the far field concentration, $C = 1$, are very small. The bulk surfactant concentration at the interface remains nearly uniform because, for Da$=0.1$, the diffusive flux of surfactant in the bulk phase is large enough to quickly eliminate any surfactant concentration gradients that may develop near the interface. Although this is generally the case for *sorption-controlled* mass transfer, the Biot number is sufficiently large in this case to allow rapid desorption of surfactants from the interface so that the surfactant flux is limited by neither bulk-phase diffusion nor interfacial desorption. The corresponding interfacial tension distributions shown in Fig. 14(c) confirm that interfacial tension gradients (and hence Marangoni stresses) have been dramatically reduced for the case of the bulk-soluble surfactant.

We conclude by showing the effect of bulk-solubility of surfactants on the marginal stability diagram. Figure 15 presents the marginal stability curves for Langmuir ($\xi = 0$) and strongly-cohesive ($\xi = -4$) surfactants, where the labels ''I'' and ''S'' are used to denote the bulk-insoluble and the bulk-soluble surfactant cases, respectively. As in the case of the insoluble surfactants, the marginal stability curves specifying the critical Bond number as a function of the initial shape perturbation, Δ, are presented at a fixed value of $\mathrm{Pe}_s = 10$. It should be noted, however, that the Bond number in Fig. 15 is based on the equilibrium value of the interfacial

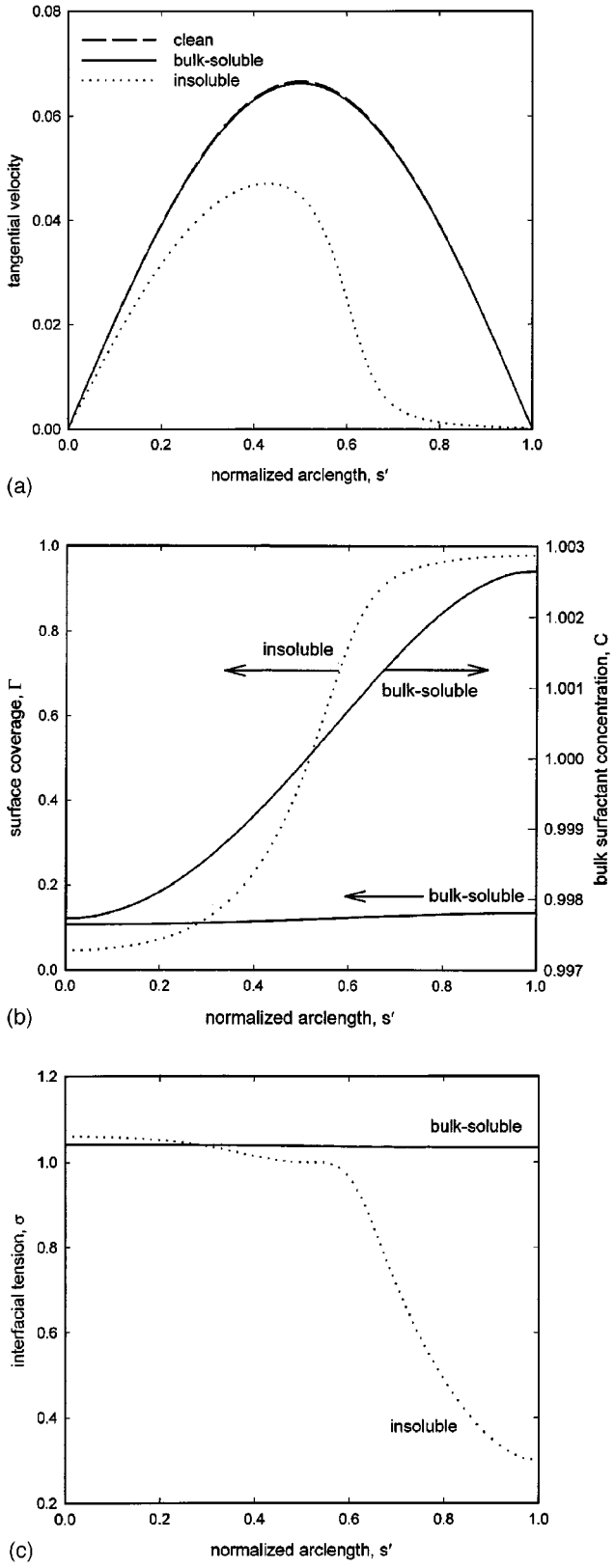

FIG. 14. The steady-state surface velocity (a), surfactant concentration (b), and interfacial tension (c) distributions for stable surfactant-laden drops with $\mathrm{Bo}_c = 2.0$, $\xi = -4$, $\mathrm{Pe}_s = 50$, Bi$=1.0$, and Da$=0.1$.

tension. In general, drops translating in the presence of bulk-soluble surfactants are more stable than those contaminated with insoluble surfactants in the sense that the critical Bond numbers at fixed values of Δ are smaller in the latter case,

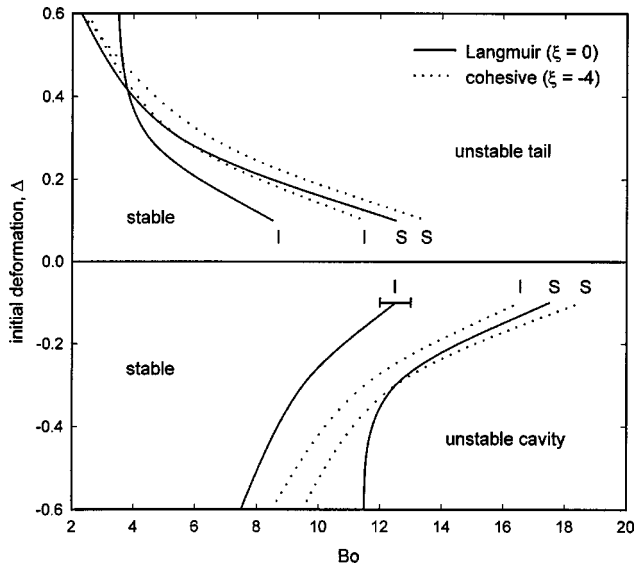

FIG. 15. The marginal stability diagram for drops translating in the presence of surfactants with $Pe_s=10$, $Da=1.0$, and $Bi=0.1$. the labels ''I'' and ''S'' denote bulk-insoluble and bulk-soluble surfactants, respectively.

except for highly-prolate initial deformations with $\Delta>0.4$. The stabilizing effect of bulk solubility is more pronounced for initially-oblate deformations ($\Delta<0$) than for initially-prolate deformations ($\Delta>0$). As in the case of insoluble surfactants, strongly-cohesive interactions have a stabilizing effect on the drop shape, although this effect is less pronounced for bulk-soluble surfactants due to the smaller surface concentrations encountered.

ACKNOWLEDGMENTS

Acknowledgement is made to the Donors of the Petroleum Research Fund, administered by the American Chemical Society, for partial support of this research.

[1]R. Clift, J. R. Grace, and M. E. Weber, *Bubbles, Drops, and Particles* (Academic, New York, 1978).
[2]T. D. Taylor and A. Acrivos, ''On the deformation and drag of a falling viscous drop at low Reynolds number,'' J. Fluid Mech. **18**, 466 (1964).
[3]M. Kojima, E. J. Hinch, and A. Acrivos, ''The formation and expansion of a toroidal drop moving in a viscous fluid,'' Phys. Fluids **27**, 19 (1984).
[4]C. J. Koh and L. G. Leal, ''The stability of drop shapes for translation at zero Reynolds number through a quiescent fluid,'' Phys. Fluids A **1**, 1309 (1989).
[5]C. J. Koh and L. G. Leal, ''An experimental investigation on the stability of viscous drops translating through a quiescent fluid,'' Phys. Fluids A **2**, 2103 (1990).
[6]C. Pozrikidis, ''The instability of a moving viscous drop,'' J. Fluid Mech. **210**, 1 (1990).
[7]H. A. Stone, ''Dynamics of drop deformation and breakup in viscous fluids,'' Annu. Rev. Fluid Mech. **26**, 65 (1994).
[8]A. Frumkin and V. Levich, Zh. Fiz. Khim. **21**, 1183 (1947).
[9]P. Savic, ''Circulation and distortion of liquid drops falling through a viscous medium,'' Nat. Res. Counc. Can., Div. Mech. Engng. Rep. MT-22, 1953.
[10]R. E. Davis and A. Acrivos, ''The influence of surfactants on the creeping motion of bubbles,'' Chem. Eng. Sci. **21**, 681 (1966).
[11]J. F. Harper, ''The motion of drops and bubbles through liquids,'' Adv. Appl. Mech. **112**, 59 (1972).
[12]J. F. Harper, ''On bubbles with small immobile adsorbed films rising in liquids at low Reynolds numbers,'' J. Fluid Mech. **58**, 539 (1973).
[13]J. F. Harper, ''Surface activity and bubble motion,'' Appl. Sci. Res. **38**, 343 (1982).
[14]S. S. Sadhal and R. E. Johnson, ''Stokes flow past bubbles and drops partially coated with thin films. Part I. Stagnant cap of surfactant films: exact solution,'' J. Fluid Mech. **126**, 237 (1983).
[15]H. N. Oguz and S. S. Sadhal, ''Effects of soluble and insoluble surfactants on the motion of drops,'' J. Fluid Mech. **194**, 563 (1988).
[16]Z. He, C. Maldarelli, and Z. Dagan, ''The size of stagnant caps of bulk soluble surfactants on interfaces of translating fluid droplets,'' J. Colloid Interface Sci. **146**, 446 (1991).
[17]V. G. Levich, *Physicochemical Hydrodynamics* (Prentice Hall, Englewood Cliffs, NJ, 1962).
[18]M. L. Wasserman and J. C. Slattery, ''Creeping flow past a fluid globule when a trace of surfactant is present,'' AIChE. J. **15**, 533 (1969).
[19]M. D. Levan and J. Newman, ''The effect of surfactant on terminal and interfacial velocities of a bubble or drop,'' AIChE. J. **22**, 695 (1976).
[20]J. A. Holbrook and M. D. Levan, ''Retardation of droplet motion by surfactant. Part 2. Numerical solutions for exterior diffusion, surface diffusion, and adsorption kinetics,'' Chem. Eng. Commun. **20**, 273 (1983).
[21]J. Chen and K. J. Stebe, ''Marangoni retardation of the terminal velocity of a settling droplet: The role of surfactant physico-chemistry,'' J. Colloid Interface Sci. **178**, 144 (1996).
[22]H. A. Stone, ''A simple derivation of the time-dependent convective-diffusion equation for surfactant transport along a deforming interface,'' Phys. Fluids A **2**, 111 (1990).
[23]R. Aris, *Vectors, Tensors, and the Basic Equations of Fluid Mechanics* (Prentice–Hall, Englewood Cliffs, NJ, 1962).
[24]C. H. Chang and E. Franses, ''Adsorption dynamics of surfactant at the air–water interface: a critical review of mathematical models, data and mechanisms,'' Colloids Surf., A **100**, 1 (1995).
[25]J. K. Ferri and K. J. Stebe, ''Soluble surfactants undergoing surface phase transitions: A Maxwell construction and the dynamic surface tension,'' J. Colloid Interface Sci. **209**, 1 (1999).
[26]R. A. Johnson, Ph.D. thesis, The Pennsylvania State University, 1999.